

Polyplex Formation between PEGylated Linear Cationic Block Copolymers and DNA: Equilibrium and Kinetic Studies

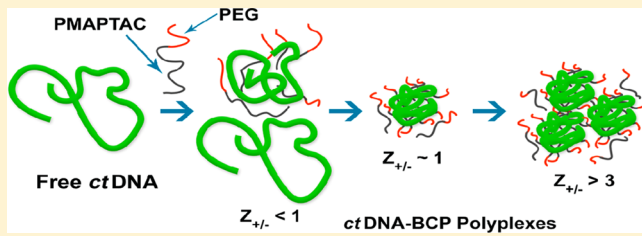
Debabrata Dey,[†] Santosh Kumar,[‡] Rakesh Banerjee,[†] Souvik Maiti,[‡] and Dibakar Dhara^{*,†}

[†]Department of Chemistry, Indian Institute of Technology Kharagpur, West Bengal 721302, India

[‡]Proteomics and Structural Biology Unit, Institute of Genomics and Integrative Biology, CSIR, Mall Road, Delhi 110007, India

S Supporting Information

ABSTRACT: The basic requirement for understanding the nonviral gene delivery pathway is a thorough biophysical characterization of DNA polyplexes. In this work, we have studied the interactions between calf-thymus DNA (*ct*DNA) and a new series of linear cationic block copolymers (BCPs). The BCPs were synthesized via controlled radical polymerization using [3-(methacryloylamino)propyl]-trimethylammonium chloride (MAPTAC) and poly(ethylene glycol) methyl ether (PEGMe) as comonomers. UV-visible spectroscopy, ethidium bromide dye exclusion, and gel electrophoresis study revealed that these cationic BCPs were capable of efficiently binding with DNA. Steady-state fluorescence, UV melting, gel electrophoresis, and circular dichroism results suggested increased binding for BCPs containing higher PEG. Hydrophobic interactions between the PEG and the DNA base pairs became significant at close proximity of the two macromolecules, thereby influencing the binding trend. DLS studies showed a decrease in the size of DNA molecules at lower charge ratio (the ratio of "+" charge of the polymer to "-" charge of DNA) due to compaction, whereas the size increased at higher charge ratio due to aggregation among the polyplexes. Additionally, we have conducted kinetic studies of the binding process using the stop-flow fluorescence method. All the results of BCP–DNA binding studies suggested a two-step reaction mechanism—a rapid electrostatic binding between the cationic blocks and DNA, followed by a conformational change of the polyplexes in the subsequent step that led to DNA condensation. The relative rate constant (k'_1) of the first step was much higher compared to that of the second step (k'_2), and both were found to increase with an increase in BCP concentration. The charge ratios as well as the PEG content in the BCPs had a marked effect on the kinetics of the DNA–BCP polyplex formation. Introduction of a desired PEG chain length in the synthesized cationic blocks renders them potentially useful as nonviral gene delivery agents.



INTRODUCTION

In recent years, nonviral gene delivery has gained immense scientific interest for its utility in treatment of critical genetic deficiencies and life-threatening diseases like cancer.^{1,2} In spite of a high efficiency of viral vectors in gene transfection, there are safety issues arising from a potential induction of immunogenic response *in vivo*. This has led to increased research focus on the nonviral delivery systems,^{3–5} e.g., cationic polymers and lipid based gene delivery vectors.^{6–8} Several classes of cationic polymers have been studied as promising nonviral vectors for facilitating the delivery and expression of DNA into cells.^{9,10} Spontaneous formation of DNA–polycation complexes (polyplexes) occurs in aqueous medium as a result of electrostatic attraction between the negatively charged phosphate groups of DNA with the positively charged centers on the polymer. This reduces the exposure of DNA to enzymes, thereby increasing its stability and the possibility of reaching the nucleus without degradation.^{11,12} Moreover, the large number of counterions released in the solution during the electrostatic interaction makes this process entropically favorable.¹³

Despite all the above advantages, DNA–polyelectrolyte polyplexes have some serious drawbacks; e.g., these electro-

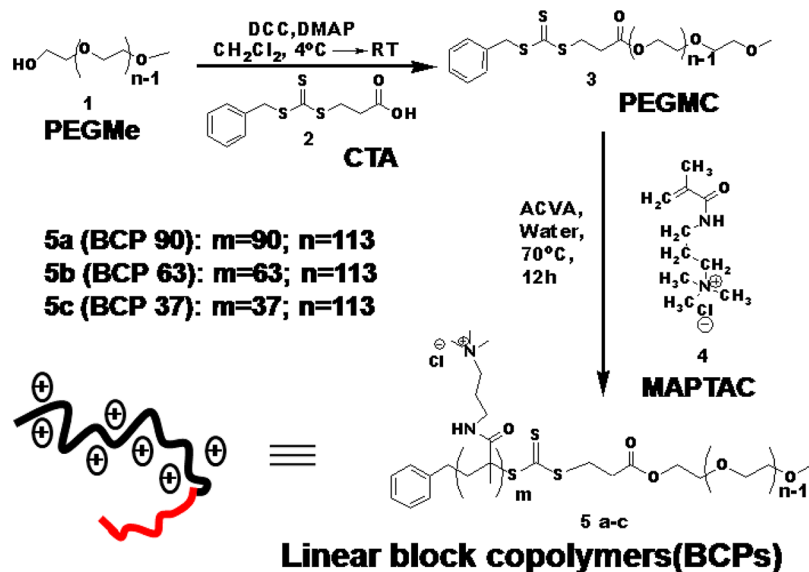
neutral polyplexes become hydrophobic in nature, form large aggregates, and precipitate out. Moreover, cationic polymers are usually toxic in nature.¹¹ Thus, the successful utilization of polyplexes in gene therapy is still a challenge. In order to meet this challenge, a detailed biophysical characterization of the complexes is required so as to understand the means of improving the transfection. Small changes in the nature, architecture, and charge density of the cationic polymers may dramatically alter the complexation process, lifetime, *in vivo* distribution, and transfection efficacy of the complexes.^{14–16} In the literature, common cationic polymers, e.g., polylysine, poly(ethylenimine), and poly(amidoamine) dendrimers, have been frequently reported for studying the DNA–polymer interactions.^{17–20} It has been observed that incorporation of glucose molecules like dextran and hydrophilic polymers like poly(ethylene glycols) (PEG) leads to remarkable improvement in the solubility, stability, cell survival, and biodistribution of the polyplexes.^{21–23} The hydrophilic shells at the polyplex

Received: February 4, 2014

Revised: May 29, 2014

Published: May 30, 2014

Scheme 1. RAFT Polymerization-Based Synthetic Route for Different PEGylated Linear Cationic Block Copolymers (BCPs), Where the Number of MAPTAC Units Was Systematically Varied to Result in Three Diblock Copolymers (5a–c)^a



^a A schematic representation of PEGylated cationic block copolymers containing different block lengths of cationic MAPTAC unit (represented by curved black lines with positive charges) and fixed block length of PEG unit (represented by curved red lines) is shown in the Bottom left.

surface were found to increase solubility, prevent aggregation due to steric repulsion, and reduce nonspecific interactions with other biomolecules and blood components, thereby extending the systemic circulation.^{11,24,25} It is a well-accepted fact that the polymer–DNA interaction is mainly electrostatic in nature where the chemical structure, geometric arrangement, and chain length of the polymer play a major role in the formation of the said complexes. Moreover, the number and spacing of the cationic charges in the polymeric chain profoundly influence the size of the polyplexes resulting from the DNA–polyelectrolyte complexation.^{11,26} It is believed that the synthesis of cationic polymers with proper and useful architecture is one of the most important aspects in the designing of a polymer-based gene delivery system. In this regard, block copolymers are particularly interesting, as they have the properties of each of the constituent homopolymer blocks as well as a unique set of properties owing to the overall polymer structure. In addition, the hydrophilic–hydrophobic balance can be maintained more efficiently in block copolymers due to the feasibility of controlling the length of either the hydrophilic or hydrophobic blocks via the controlled polymerization technique.²⁷

In this work, we have synthesized a series of linear block copolymers (BCPs) using [3-(methacryloylamino propyl)]-trimethylammonium chloride (MAPTAC) and poly(ethylene glycol) methyl ether ($M_n = 5000$) (PEGMe) as comonomers via the RAFT polymerization technique^{28,29} and investigated their interaction with calf-thymus DNA (ctDNA). Techniques like steady-state fluorescence spectroscopy, temperature dependent UV melting of DNA, agarose gel electrophoresis, DLS, and circular dichroism (CD) were performed in order to understand the effect of the polymer architecture on the DNA–polymer interaction at the molecular level.

In the second part of our investigation, we have conducted a kinetic study of the block copolymer–DNA polyplex formation process. We have tried to correlate the kinetic parameters that control the compaction process of DNA in the presence of

cationic block copolymers with variation in polymer compositions. This information is important in connection to gene transport considering the fact that the release of DNA from the vectors has a profound kinetic implication. In fact, the lifetime of the polyplexes and their dissociation *in vivo* plays an important role in determining their efficiency. We have used the stopped-flow fluorescence technique for the kinetic studies, as it allows a rapid and automatic mixing of the sample and the reagent solutions, followed by instantaneous measurements after the mixing.³⁰ We believe that this series of cationic poly(MAPTAC)–PEG block copolymers has the potential to be used as a model system for understanding the mechanism of the DNA–cationic polymer interactions. Moreover, the biophysical studies with this series of PEGylated cationic BCPs may help in designing novel and superior gene transfer vectors. To the best of our knowledge, this work is the first attempt toward understanding simultaneously the equilibrium as well as the kinetic behavior of a nucleic acid–PEGylated cationic BCP system. Such a complete biophysical study is important for gathering detailed insight into designing novel polyplexes.

MATERIALS AND METHODS

Materials. Sodium salt of ctDNA, poly(ethylene glycol) methyl ether ($M_n = 5000$) (PEGMe), ethidium bromide (3,8-diamino-5-ethyl-6-phenylphenanthridium bromide, EB), and 4,4'-azobis (4-cyanovaleic acid) (ACVA) were purchased from Sigma-Aldrich and used without further purification. [3-(Methacryloylamino) propyl]trimethylammonium chloride (MAPTAC, 50% in water) was obtained from Sigma-Aldrich and was passed through a neutral alumina column to remove the inhibitor and stored at -20°C before use. 3-(Benzylthiocarbonothioylthio) propanoic acid was prepared according to a reported procedure, with slight modification.³¹ All of the experiments were carried out using 10 mM potassium phosphate buffer (pH 7.4), prepared in Milli-Q water. All other chemicals used in this study were of AR grade purity and used

as received. Unless otherwise specified, the concentrations of DNA solutions are given in molarity units in terms of negatively charged phosphate groups in the DNA backbone.

Synthesis of 3-(Benzylthiocarbonothioylthio) Propanoic Acid. 3-(Benzylthiocarbonothioylthio) propanoic acid was synthesized following the reported procedure³¹ with some modification. The details of the synthesis procedure followed and characterization are given in the Supporting Information.

Synthesis of PEGMe Macro-CTA (PEGMC). The synthesis of PEGMe macro-CTA (PEGMC) was carried out following the reported procedure³² with some modification, as depicted in Scheme 1. The details of the synthesis process and characterization are given in the Supporting Information.

Synthesis of PMAPTAC-*b*-PEG₅₀₀₀ Diblock Copolymers, BCPs. PEGMC of $M_n \sim 5250$ (1 g, 0.19 mmol) and an appropriate amount of cationic monomer MAPTAC were taken in 15 mL of Milli-Q water in a 25 mL dried RB flask. Three different block copolymers were synthesized using a MAPTAC to PEGMC mole ratio of 100:1, 65:1, and 40:1, keeping the PEGMC to initiator, i.e., 4,4'-azobis (4-cyanovaleric acid) (ACVA), mole ratio fixed at 4:1. Oxygen was removed from the reactor by purging nitrogen gas for 30 min. Thereafter, the reaction mixture was kept in a preheated oil bath maintained at 70 °C and the polymerization reactions were carried out for 12 h before terminating by immersion of the reaction flask in liquid nitrogen. The block copolymer products were dialyzed (mol. wt. cutoff 7000 Da) against Milli-Q water for 3 days, freeze-dried, and characterized by ¹H and ¹³C NMR. As a sample for comparative study, poly(MAPTAC) homopolymer (PMAPTAC) of $M_n = 18\,000$ was prepared by controlled synthesis of MAPTAC at 70 °C using V-501 as the primary radical source and 4-cyanopentanoic acid dithiobenzoate as the chain-transfer agent.³³

Preparation of BCP-*c*tDNA Polyplexes. The BCP-DNA polyplexes were prepared by adding the required amount of polymer solution to the *c*tDNA solution in 10 mM potassium phosphate buffer (pH ~ 7.4) in order to achieve an appropriate polymer to DNA charge ratio ($Z_{+/-}$) followed by vortexing and equilibration for 1 h. The $Z_{+/-}$ ratio was expressed via the ratio of equivalents of cationic MAPTAC units (from NMR results) to the number of negatively charged phosphate groups in DNA. The concentration of DNA stock solution was measured by a Cary 100 UV-visible spectrophotometer. The concentration of *c*tDNA (in terms of negatively charged phosphate group) was measured by its absorbance at 260 nm with a molar extinction coefficient (ϵ) of 6600 M⁻¹ cm⁻¹. The concentration of DNA in terms of base pairs is exactly half the concentration of phosphate groups ($\epsilon = 13\,200$ M⁻¹ cm⁻¹). The ratio of the absorbance of DNA solution at 260 and 280 nm was 1.82, and the absorbance at 320 nm was negligible, confirming the absence of any protein contamination. The stock solution of EB was prepared by dissolving 2.2 mg in 1 mL of phosphate buffer. The concentration was determined by using an UV-visible spectrophotometer ($\epsilon = 5600$ M⁻¹ cm⁻¹ at 480 nm). EB solutions were stored in the dark at 4 °C before use. The BCP stock solutions (5150 μM) were prepared by dissolving a known weight of each BCP in a required volume of phosphate buffer solution.

UV Spectroscopy and Turbidity Measurement. UV-vis absorption spectra were recorded between 200 and 600 nm wavelength using a Shimadzu UV-2450 UV spectrophotometer. The concentration of *c*tDNA was 25 μM in terms of negatively charged phosphate groups. The addition of BCP solutions

continued so that the charge ratio was varied from $Z_{+/-} = 0$ to $Z_{+/-} = 9$; no turbidity was visually observed in this entire range $Z_{+/-}$.

Steady-State Fluorescence Spectroscopic Studies.

Steady-state fluorescence spectra were taken in a Jobin Yvon Fluorolog spectrofluorometer. The excitation wavelength was 480 nm, and the emission spectra were taken from 500 to 700 nm wavelength range. The excitation slit and emission slit were fixed at 5 and 2 nm, respectively. The temperature was set at 25 °C. For making the DNA-EB complex, the DNA stock solutions and EB stock solutions were mixed (1 EB:1 bp) in the phosphate buffer and equilibrated for 10 min. To a *c*tDNA-EB mixture (1 mL) in a quartz cuvette, the desired amounts of BCP stock solutions were added. After addition of a given BCP solution, the resultant mixture was equilibrated for 10 min before recording the steady-state fluorescence spectrum. The working concentration range of *c*tDNA in steady-state fluorescence spectroscopy was the same as that used in UV-vis measurements.

Agarose Gel Electrophoresis. The electrophoretic mobility of the BCP-DNA complexes at different $Z_{+/-}$ values was studied by gel electrophoresis using 0.8% agarose gel mixed with 30 μg of ethidium bromide in a buffer consisting of 40 mM Tris-borate and 1 mM EDTA at pH 8.0. Experiments were run at 80 V for 90 min. DNA was visualized under UV illumination (254 nm).

Circular Dichroism (CD) Spectroscopy. The changes in the conformations of the polymer-complexed DNA relative to free DNA were determined by analysis of their CD spectra. The CD spectra were obtained at 25 °C using a JASCO 815 (Japan) instrument. Typically, a solution of 100 μM *c*tDNA in 10 mM phosphate buffer was titrated with the appropriate BCP solution in 10 mM phosphate buffer from $Z_{+/-} = 0$ to $Z_{+/-} = 4$.

Measurement of the Melting Curve of BCP-DNA Polyplexes. Free *c*tDNA was dissolved in 10 mM potassium phosphate buffer (pH 7.4) to achieve a final concentration of 25 μM. Different volumes of BCP solutions were separately added to a constant volume of DNA solution to obtain BCP-DNA polyplexes of different charge ratios. After 1 h of incubation at room temperature, the melting profiles of the complexes were obtained by measuring the absorbance of the complexes at 260 nm as a function of temperature. The samples were heated from 40 to 95 °C at a scanning rate of 1.0 °C/min. Melting temperatures (T_m) have been calculated from the melting curves.

Dynamic Light Scattering (DLS) Measurements. The size and the size distribution of *c*tDNA and DNA-cationic BCP complexes have been characterized by means of dynamic light scattering measurements using a Malvern Nano ZS instrument employing a 4 mW He-Ne laser operating at a wavelength of 633 nm and an avalanche photodiode (APD) detector. The temperature was kept constant (25 °C) by circulating water through the cell holder using a JEIO TECH Thermostat (RW-0525GS). The concentration of *c*tDNA was kept fixed at 25 μM in terms of negatively charged phosphate groups. The addition of BCP solutions continued so that the charge ratio was varied from $Z_{+/-} = 0$ to $Z_{+/-} = 12$. After mixing the polymer with DNA in a cuvette, 10 min was allowed for equilibration to each sample mixture before recording the spectrum. Autocorrelation functions were deconvoluted using CONTIN software.

Stopped-Flow Fluorescence Kinetic Studies. The kinetic measurements were carried out using a SFA-20 rapid

Table 1. Composition, Molecular Weight, and Number of Cationic Units per Polymer Chain in the Synthesized Cationic Block Copolymers

polymer abbreviation	polymer composition	no. of cationic units per polymer chain estimated from theory ^a	no. of cationic units per polymer chain ^b	M_n ^b
PEGMC	PEGMe ₅₀₀₀ macro-CTA		0	5250
BCP 90	(MAPTAC) ₉₀ - <i>b</i> -PEGMe ₅₀₀₀	100	90	25 100
BCP 63	(MAPTAC) ₆₃ - <i>b</i> -PEGMe ₅₀₀₀	65	63	19 200
BCP 37	(MAPTAC) ₃₇ - <i>b</i> -PEGMe ₅₀₀₀	40	37	13 500
PMAPTAC ^c	(MAPTAC) ₈₀		80	18 000

^aConsidering 100% conversion of MAPTAC. ^bFrom ¹H NMR (400 MHz, Bruker). ^cFrom ref 33.

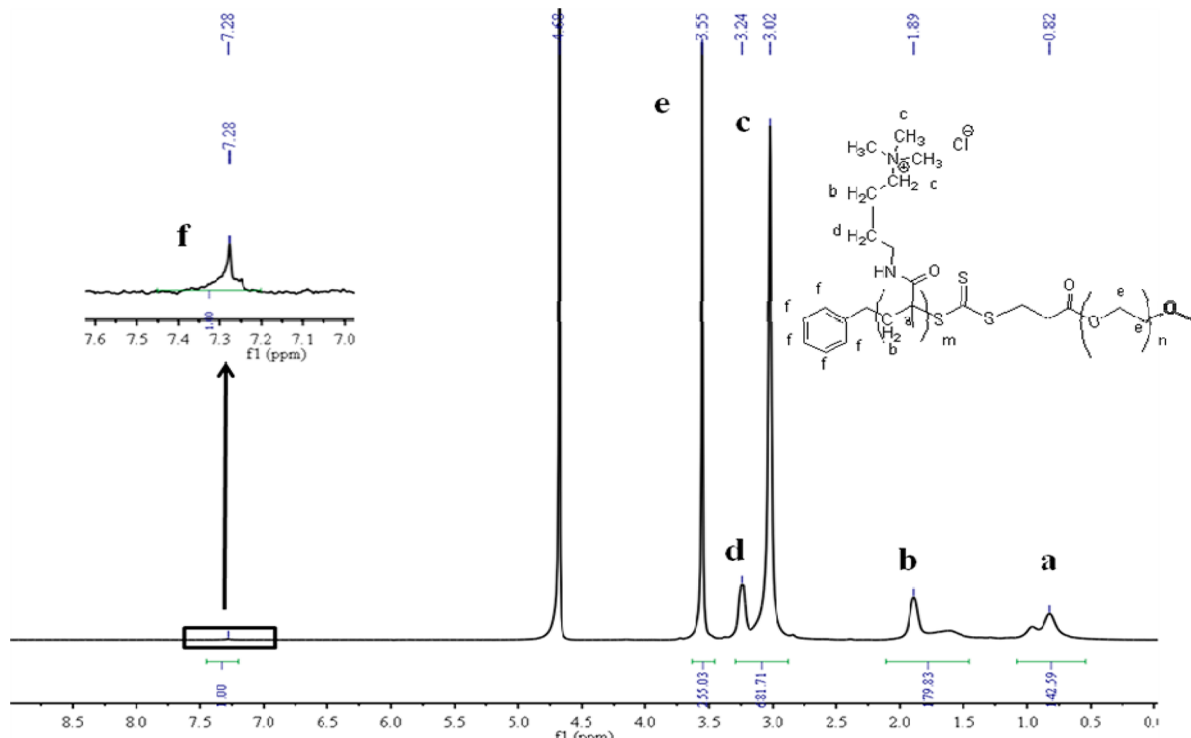


Figure 1. ¹H NMR spectra (in D₂O) of BCP 90 block copolymer of MAPTAC (90 mol %) and PEGMe (M_n = 5000, 1 mol %) [(MAPTAC)₉₀-*b*-PEGMe₅₀₀₀].

kinetics accessory (HI-Tech Scientific) in a Jobin Yvon Fluorolog with a Peltier thermostat. The concentration of *c*tDNA-EB complex solution (EB:b.p. = 1.0) was 50 μ M, and three different concentrations of the BCP solutions were used, i.e., 50, 150, and 450 μ M, to maintain the charge ratio of the resultant solutions, $Z_{+/-}$ = 1, 3, and 9, respectively, upon mixing of equal volumes of two solutions. The excitation and emission monochromator were set at 480 and 590 nm, respectively. During the experiment, two separate syringes were filled up with *c*tDNA-EB complex and BCP solutions, respectively. In each run, equal volumes of both of the solutions were injected at once into the sample chamber. The emission spectra of EB were monitored continuously both before (t = 0 s) and after the injection. The dead time of the instrument was determined from the test reaction described elsewhere³⁴ and was found to be 5 ms for a 1:1 mixture. Suitable control experiments were performed by mixing a *c*tDNA-EB complex solution and buffer solutions without BCPs. Photobleaching of the EB dye was ruled out, since the fluorescence signal of the *c*tDNA-EB complex remained unchanged with time while carrying out the control experiments.

RESULTS

Synthesis of the Block Copolymers. A series of cationic block copolymers of MAPTAC and PEGMe (M_n = 5000) were synthesized by the RAFT polymerization technique, as shown in Scheme 1. In the first step, PEGMe (M_n = 5000) was coupled with 3-(benzylthiocarbonothioylthio) propanoic acid to form a macro chain transfer agent (PEGMC) which was then used for polymerization of MAPTAC in the subsequent step to form the desired block copolymers. In order to confirm the effect of PEG, a comparative study was also done using a PMAPTAC homopolymer which was synthesized by RAFT polymerization, as described in our previous work.³³ Synthesis of the block copolymerization was performed in Milli-Q water with three different ratios of the MAPTAC to PEGMC in order to get block copolymers with different block lengths of PMAPTAC. Thus, all the block copolymers under investigation have the same PEG block length but different PMAPTAC block lengths.

The composition and the molecular weight of the polymers are given in Table 1. ¹H NMR spectra of one of the block copolymers BCP 90, (MAPTAC)₉₀-*b*-PEGMe₅₀₀₀, is shown in Figure 1. ¹H NMR spectra of the other two block copolymers

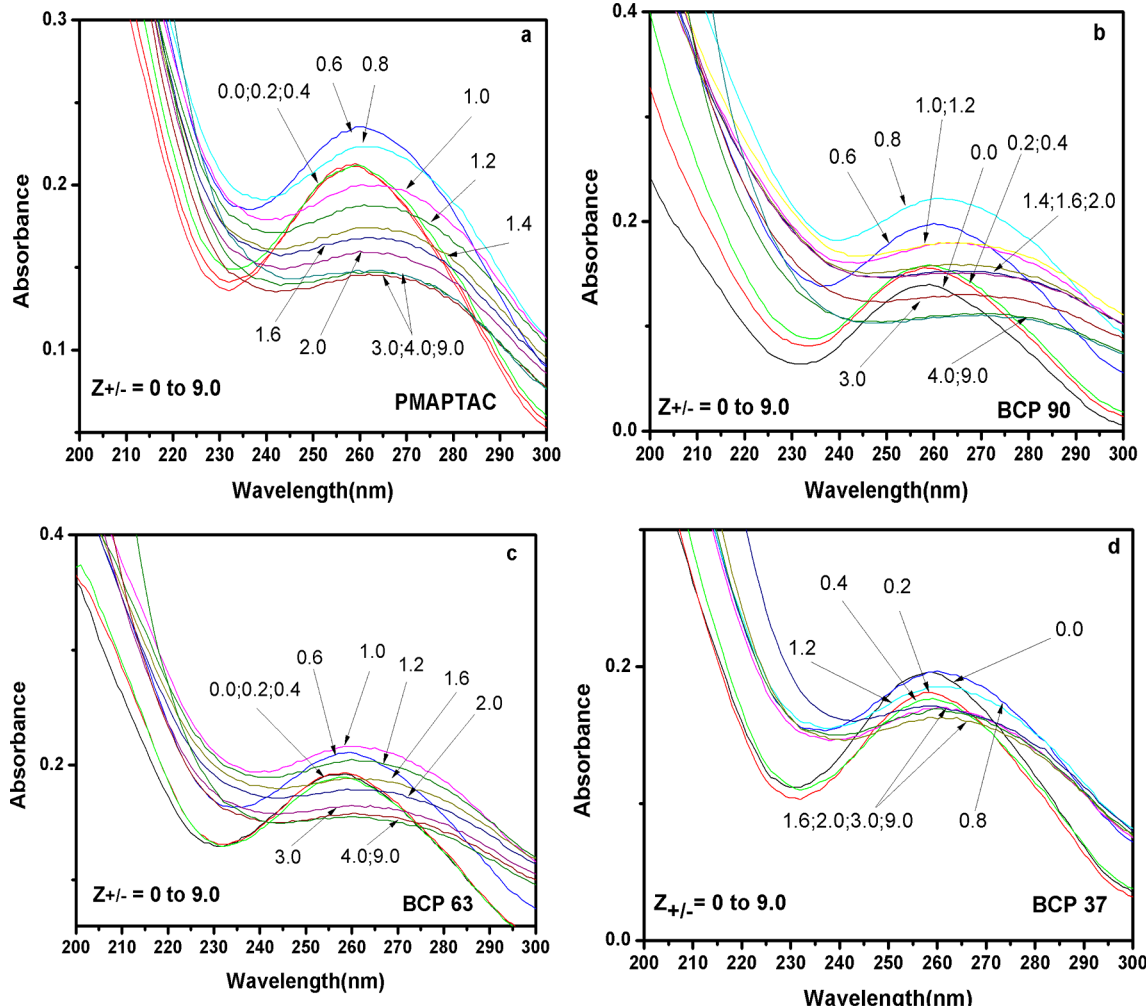


Figure 2. UV spectra of ctDNA–BCP solutions at different charge ratio $Z_{+/-}$, as shown by the arrows: (a) PMAPTAC; (b) BCP 90; (c) BCP 63; (d) BCP 37.

are shown in the Supporting Information (Figure S3a,b). We have used the molecular weight data obtained from ^1H NMR spectra for calculation of charge ratios and concentration of the polymers in solutions, as this method of determination of polymer molecular weight provides absolute and also more reliable number-average molecular weight data for quantification. The copolymer compositions and molecular weights were determined by ^1H NMR spectroscopy (400 MHz, Bruker) using D_2O as NMR solvent. The compositions of the block copolymers were determined by integration of relative intensities of methylene protons adjacent to ester oxygen of the PEGMe block with chemical shift value at 3.55 ppm and intensities of the protons adjacent to the quaternary nitrogen in the PMAPTAC block with chemical shift value at 3.02 ppm. GPC traces of all three BCPs with 1% NaCl as eluent showed a monomodal distribution.

UV Absorption Spectra. To monitor the change in the spectra of ctDNA in solution following the addition of different BCPs, the absorption spectra of different compositions of DNA–BCPs were recorded from 200 to 300 nm wavelength at various charge ratios $Z_{+/-}$. Figure 2 shows that with the addition of cationic BCPs to ctDNA solution until $Z_{+/-} = 0.4$ there was no significant change in the spectral pattern. On further increase in $Z_{+/-}$ value up to $\sim Z_{+/-} = 1.0$, the absorbance values at 260 nm increased with a slight red shift of the λ_{\max} .

This may be due to the presence of both free and complexed DNA in the mixture. A similar increase in UV absorption was reported for the PAMAM–DNA system earlier.³⁵ On addition of BCPs beyond $Z_{+/-} \sim 1.0$, the spectral patterns of the DNA–BCP complexes were found to be changed with a simultaneous decrease in UV absorption. The shifting of UV absorption maxima from 260 nm to 275 nm with a concomitant decrease in UV absorption suggests that at higher $Z_{+/-}$ values no free DNA remained in the solution and conformational transition of free DNA helix to compact globule structure of DNA.

Steady-State Fluorescence and Ethidium Bromide Exclusion Assay. The binding between cationic BCPs and ctDNA was confirmed from the fact that ethidium bromide (EB), an intercalating dye, was effectively displaced from the DNA by the cationic agents. It is known that EB binds to DNA by intercalation into the base pairs, thereby stretching the double helix of DNA that illuminates under fluorescence.²⁰ Here, the formation of BCP–DNA polyplexes was studied by following the reduction in the fluorescence intensity as EB molecules were displaced. As shown in Figure 3a,b (and in Figure S4, Supporting Information), the fluorescence of EB–DNA complexes decreased as BCPs were added, suggesting that the DNA–BCP interaction was sufficiently strong to displace a significant quantity of EB. It was observed that the BCP 37 block displaced the highest amount of EB (98% at $Z_{+/-}$

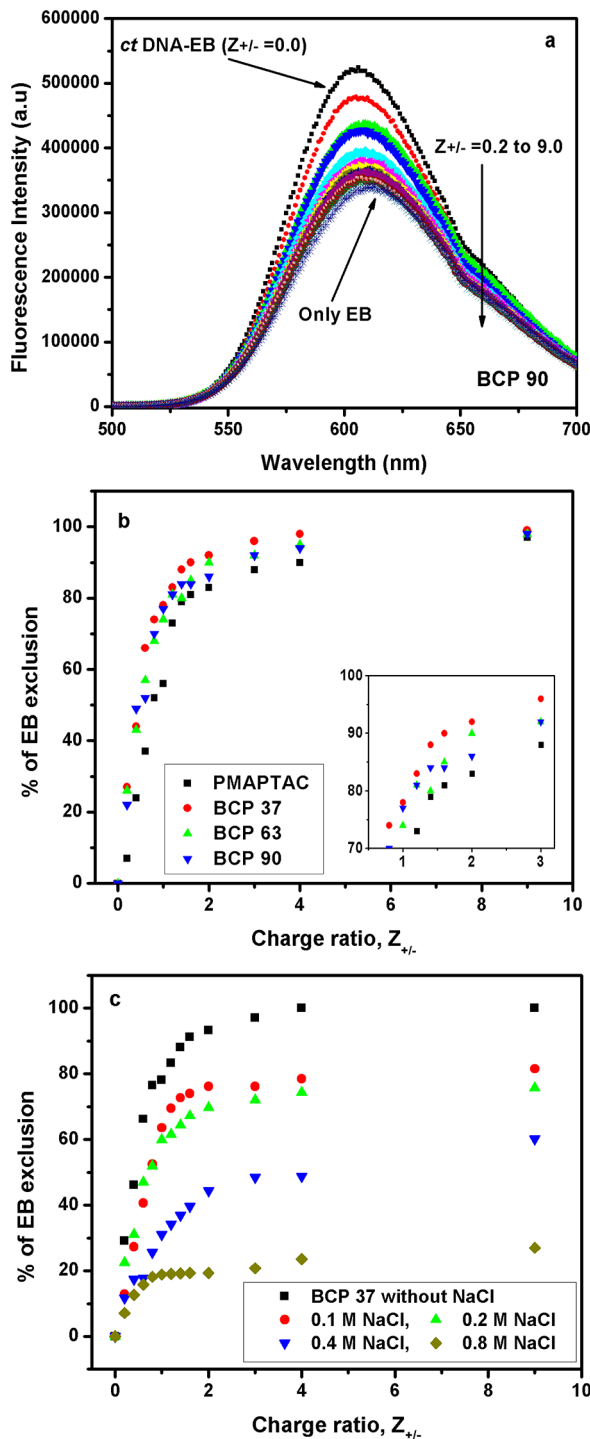


Figure 3. (a) Fluorescence spectra of ethidium bromide (EB)–DNA complex in the presence of various amounts of BCP 90; traces for fluorescence emission spectra of free EB and EB bound to *ct*DNA are marked by arrows. Percentage of EB exclusion from *ct*DNA–EB complex in the presence of (b) various cationic polymers and (c) BCP 37 at different concentrations of NaCl salt.

$= 4$) while PMAPTAC displaced the lowest amount of EB (90%, at $Z_{+-} = 4$) in the series, at the same charge ratio. Thus, the relative binding affinity of the cationic BCPs followed the order: BCP 37 > BCP 63 > BCP 90 > PMAPTAC which correlated quite well with their PEG content, in spite of the electrostatic interaction being the major contributing factor in the BCP–DNA binding process. To confirm the electrostatic

nature of the *ct*DNA–BCP binding, an EB exclusion experiment was done in the presence of various concentrations (from 0.1 to 0.8 M) of NaCl. Figure 3c shows the EB exclusion behavior for the *ct*DNA–BCP 37 polyplex. As the concentration of salt was increased, the interaction among polymer–DNA became weak. Interlaced EB in DNA helix is partially excluded by cationic polymer at higher salt concentration. This proves that *ct*DNA–BCP interaction is mainly electrostatic in nature, which becomes weak in the presence of high salt concentration.

We have used EB exclusion curves to determine the binding constants and free energy change due to DNA–cationic polymer complex formation following previously reported literature.¹¹ The concentration of cationic polymers required to exclude 50% ethidium bromide can provide a qualitative comparison between the binding constants of the copolymers with *ct*DNA.¹¹ The following equation has been used to calculate the binding constants and free energy changes

$$\begin{aligned} K_{\text{EB}} C_{\text{EB}} &= K_{\text{PMAPTAC}} C_{\text{PMAPTAC-50\%}} = K_{\text{BCP 90}} C_{\text{BCP 90-50\%}} \\ &= K_{\text{BCP 63}} C_{\text{BCP 63-50\%}} = K_{\text{BCP 37}} C_{\text{BCP 37-50\%}} \end{aligned} \quad (1)$$

K_{EB} is the binding affinity of ethidium bromide for *ct*DNA and was taken as $2.8 \times 10^5 \text{ M}^{-1}$ at 25°C from a previously reported value.¹¹ C_{EB} is the concentration of EB dye used in the study ($12.5 \mu\text{M}$). K_{PMAPTAC} , $K_{\text{BCP 90}}$, $K_{\text{BCP 63}}$, and $K_{\text{BCP 37}}$ are the binding constants of PMAPTAC, BCP 90, BCP 63, and BCP 37, respectively, with *ct*DNA. $C_{\text{PMAPTAC-50\%}}$, $C_{\text{BCP 90-50\%}}$, $C_{\text{BCP 63-50\%}}$, and $C_{\text{BCP 37-50\%}}$ are the concentrations (in terms of cationic charge) needed to exclude 50% of bound ethidium bromide. The obtained K_{PMAPTAC} , $K_{\text{BCP 90}}$, $K_{\text{BCP 63}}$, and $K_{\text{BCP 37}}$ are presented in Table 2. The corresponding free energy

Table 2. Binding Constants and Free Energy Change Values Obtained from the Cationic Polymer–*ct*DNA Complexation Process by EB Exclusion Experiments at 25°C

cationic polymer	binding constant, K_b (M^{-1})	ΔG (kcal/mol)
PMAPTAC	1.8×10^5	-7.14
BCP 90	2.43×10^5	-7.32
BCP 63	2.92×10^5	-7.42
BCP 37	3.54×10^5	-7.54

changes of the process are calculated using the relation $\Delta G = -RT \ln K$, where ΔG is the corresponding free energy change of the process, and the values are provided in Table 2. The calculated binding affinities are of the order of 10^5 M^{-1} (in terms of cationic charge concentration) for all the polymers studied here, indicating strong binding between the *ct*DNA and BCPs. These binding affinities are of higher value compared to random copolymers of similar type of polymers.¹¹ To find out the enthalpy change during the interaction between the polymers and *ct*DNA, we have conducted a microcalorimetry study. The enthalpy changes were found to be very low (see Figure S5, Supporting Information). This corroborates that the interactions between the cationic polymers and DNA are entropically driven. During the charge neutralization process between the cationic polymer and negatively charged *ct*DNA, the large amount of counterion release contributes largely toward the entropic change of the process. Therefore, the driving force of the polyplex formation of DNA is predominantly entropy driven.

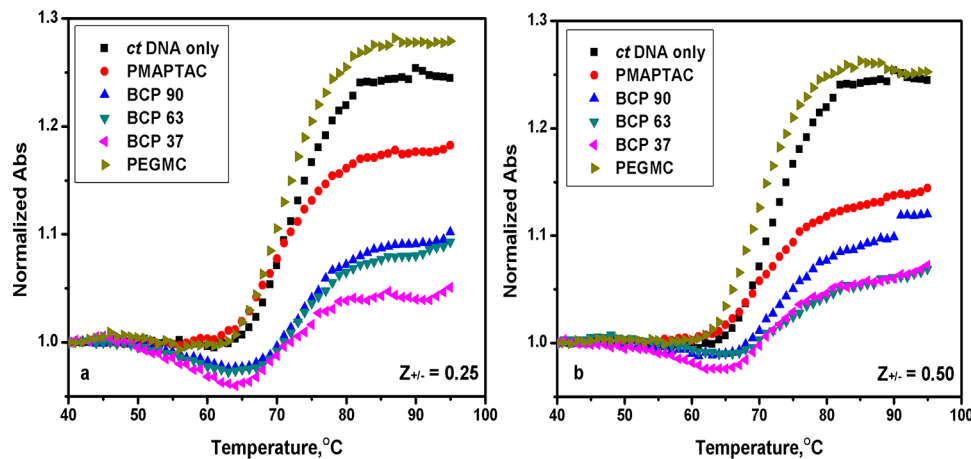


Figure 4. Comparison of UV melting profiles of BCP bound *ct*DNA complexes at different charge ratios: (a) $Z_{+/-} = 0.25$; (b) $Z_{+/-} = 0.50$.

Melting of BCP–DNA Polyplexes. The UV melting curve has been widely used for characterization of DNA polyplexes in the literature, as it can directly predict the stability of DNA polyplexes.^{11,39} DNA melting temperatures (T_m) have been determined from the melting curves in order to gain vital information about the helix–coil–globule transition. Differences observed in T_m values at various compositions of DNA–BCP complexes would directly suggest whether the presence of different BCPs at various charge ratios would impart any stability to the *ct*DNA. The melting profiles of BCP–DNA polyplexes at two different $Z_{+/-}$ values in 10 mM phosphate buffer are shown in Figure 4 and in the Supporting Information (Figure S6). The melting curves revealed biphasic sigmoidal behavior. In all of the polymer–DNA mixtures, the transition occurring around 72–73 °C was due to the melting of free DNA. The second transition corresponds to melting of polymer–DNA polyplexes existing near/above 100 °C, as indicated by the upward increase in the UV absorption at higher temperature. This is not surprising because, in the presence of cationic polymers, DNA becomes more stabilized compared to the native free DNA. On melting, normally an increase in absorbance (hyperchromic effect) is observed which could be directly related to the disruption of base stacking in double-stranded DNA due to breakage of hydrogen bonds.⁴⁰ A close inspection of melting profiles shows, in the cases of higher charge ratio, slight and gradual loss of absorption initially happened for all of the polymer–DNA mixtures. These slight initial losses of absorption suggest formation of a compact globule structure of polyplexed DNA molecules. A similar type of biphasic sigmoidal melting behavior has been reported in the literature.⁴¹

Dynamic Light Scattering (DLS) Measurements. The average hydrodynamic size and the size distribution of free *ct*DNA and DNA–cationic BCP polyplexes were studied by the DLS technique. Important information like the cationic BCP-induced conformational changes in DNA chain, size distribution of resultant DNA–polymer complexes, and occurrence of any aggregation could be obtained using the dynamic light scattering (DLS) technique. Figure 5 shows the average hydrodynamic size of a *ct*DNA solution ([DNA] = 25 μM in terms of phosphate group) in the presence and absence of cationic BCPS at different charge ratios $Z_{+/-}$. The results clearly show the existence of three different regions of average size DNA–BCP polyplexes with variation of $Z_{+/-}$. As can be seen from Figure 5, with an increase in the cationic BCP content, a

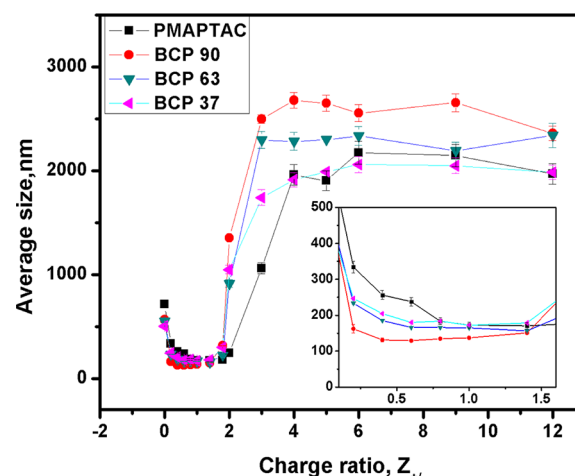


Figure 5. Average size of *ct*DNA–BCP polyplexes as obtained from dynamic light scattering measurements plotted as a function of charge ratio $Z_{+/-}$.

progressive decrease of the average size from ~700 to ~130–150 nm of the *ct*DNA–BCP mixtures occurred at the charge ratio below $Z_{+/-} \sim 1$. Beyond $Z_{+/-} \sim 1$, the average size of the polyplexes increases first slightly and then drastically to about 2000–2500 nm for charge ratio until $Z_{+/-} = 4$. On further increase of $Z_{+/-}$ values, no significant change in the average size of polyplexes was observed.

DLS histograms for one of the polymer–DNA systems, PMAPTAC–DNA, at varying charge ratios are shown in Figure 6. For other samples, DLS histograms are given in the Supporting Information (Figure S7). CONTIN software has been used for deconvolution of autocorrelation functions. As the polymer–*ct*DNA system is polydisperse in nature, the CONTIN method can provide better information regarding the size and distribution of DNA polyplexes over the cumulant method.

Agarose Gel Electrophoresis Studies. Agarose gel electrophoresis study helps to visualize the interaction of DNA with the polycations. As calf-thymus DNA is highly polydisperse in nature, we have used plasmid DNA instead of calf-thymus DNA for better understanding of the electrophoretic mobility of BCP–DNA complexes. As electrostatic interaction is the main contributing factor in the binding process of BCP–DNA systems, changing the DNA type in gel

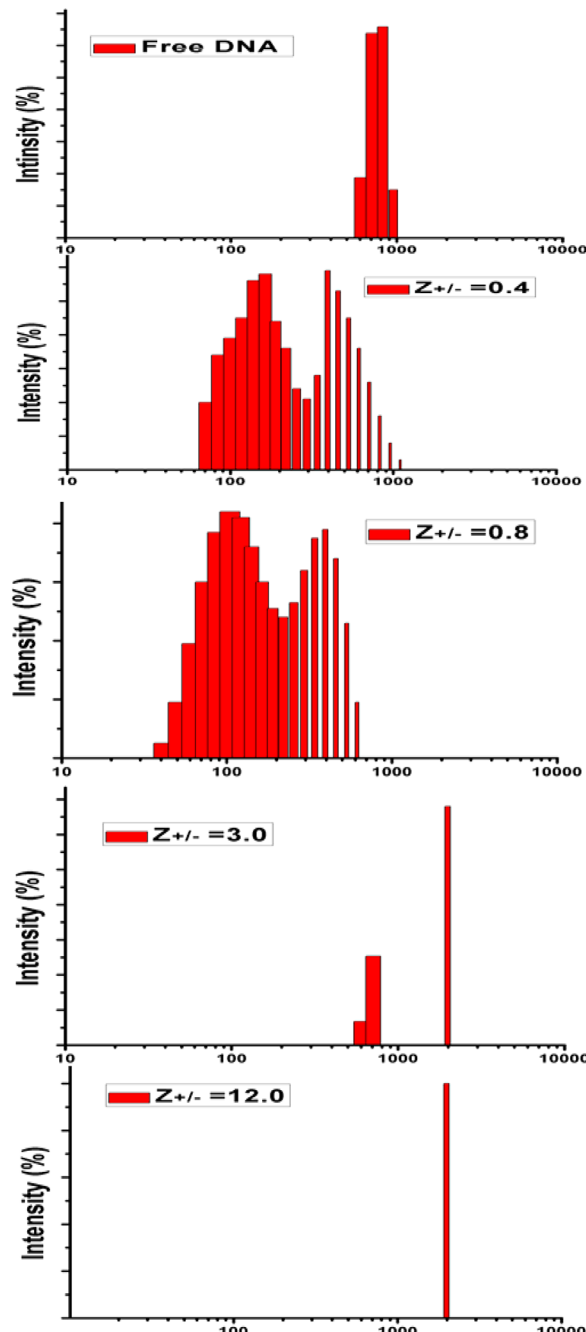


Figure 6. DLS histograms showing the intensity distribution profiles of *ct*DNA-PMAPTAC polyplexes at different charge ratios (*x*-axis: hydrodynamic diameter, nm; deconvolution of the autocorrelation function was carried out using CONTIN software).

electrophoresis study would not cause much difference in the final inference. The rather narrow, disperse nature of plasmid DNA would help us to detect the small electrophoretic mobility difference in our study. Polyplexes of plasmid DNA were formed with different BCPs at different charge ratios, and agarose gel electrophoresis was subsequently performed. The results of gel electrophoresis for all polymers are shown in Figure 7. In the cases of all the cationic block polymers including PMAPTAC, bands were observed at nearly the same distance at various charge ratios but with diminishing intensity as the $Z_{+/-}$ were increased. At higher charge ratio ($Z_{+/-} = 2.0$, lane 7), there was no observable band in the gel.

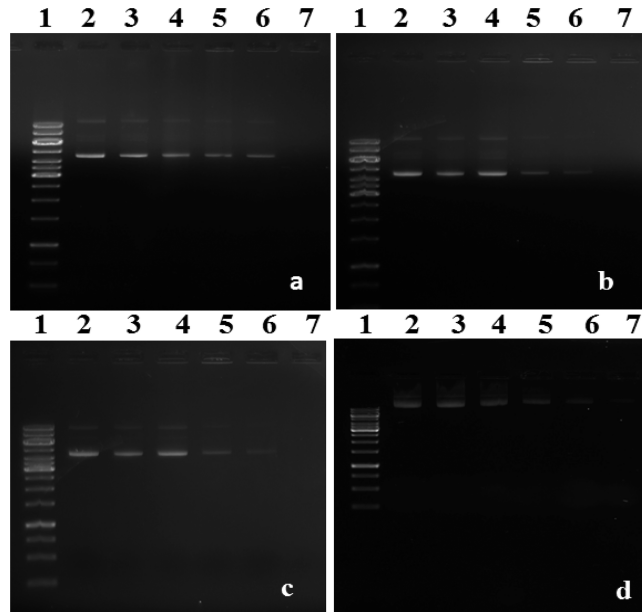


Figure 7. Agarose gel electrophoresis study of different DNA-BCP complexes at various charge ratios: (a) PMAPTAC; (b) BCP 90; (c) BCP 63; (d) BCP 37. Lane 1, standard ladder; lane 2, free DNA; lanes 3–7, polyplexes at various charge ratio: lane 3, $Z_{+/-} = 0.25$; lane 4, $Z_{+/-} = 0.50$; lane 5, $Z_{+/-} = 0.75$; lane 6, $Z_{+/-} = 1.0$; lane 7, $Z_{+/-} = 2.0$.

Circular Dichroism (CD) Spectroscopy Study. CD spectroscopy is an important tool to monitor the possible conformation changes of DNA upon complexation with cationic agents. Figure 8 shows the CD spectra of the free *ct*DNA and cationic BCP bound complexes at several $Z_{+/-}$ ratios. The free *ct*DNA is typical of a duplex in B conformation.^{36,37} The B-form conformation of *ct*DNA showed two CD bands in the UV region: a positive band at 275 nm due to base stacking and a negative band at 245 nm due to polynucleotide helicity. None of our BCPs showed any optical activity. The CD spectra of *ct*DNA showed a remarkable decrease in the positive band ellipticity at 275 nm with a red shift due to the addition of BCPs. The effect was more prominent with an increase in $Z_{+/-}$ ratio. The red shift was also observed in the negative band at 245 nm, but in this case, the change in ellipticity trend was just reversed with increasing $Z_{+/-}$. Near $Z_{+/-} = 1.0$ and above, the peaks at 275 and 245 nm were almost completely disappeared, indicating the possibility of compact globule formation of DNA polyplexes. Another notable fact is that the peak intensity changes were more prominent in the case of PMAPTAC for which PEG content was nil and relatively less variations were seen in the case of BCP 37. At a given $Z_{+/-}$, more PEG is present in the case of BCP 37 block as compared to BCP 63 or BCP 90. It is reported that simple groove binding and electrostatic interaction of the cationic agent with *ct*DNA showed perturbation of the base stacking and helicity bands, whereas its intercalation can enhance the intensities of both bands to stabilize the right-handed B conformation.^{37,38} Overall, our investigation revealed that the binding of cationic BCPs to negative phosphate groups of calf-thymus DNA induced minor perturbations in the DNA helical structure up to $Z_{+/-} \sim 1.0$ for all the BCPs.

Stopped-Flow Fluorescence Spectroscopic Studies and Kinetic Measurements. The primary requirements for a successful gene delivery agent are (i) overall charge neutralization resulting in collapse of the DNA and polycation

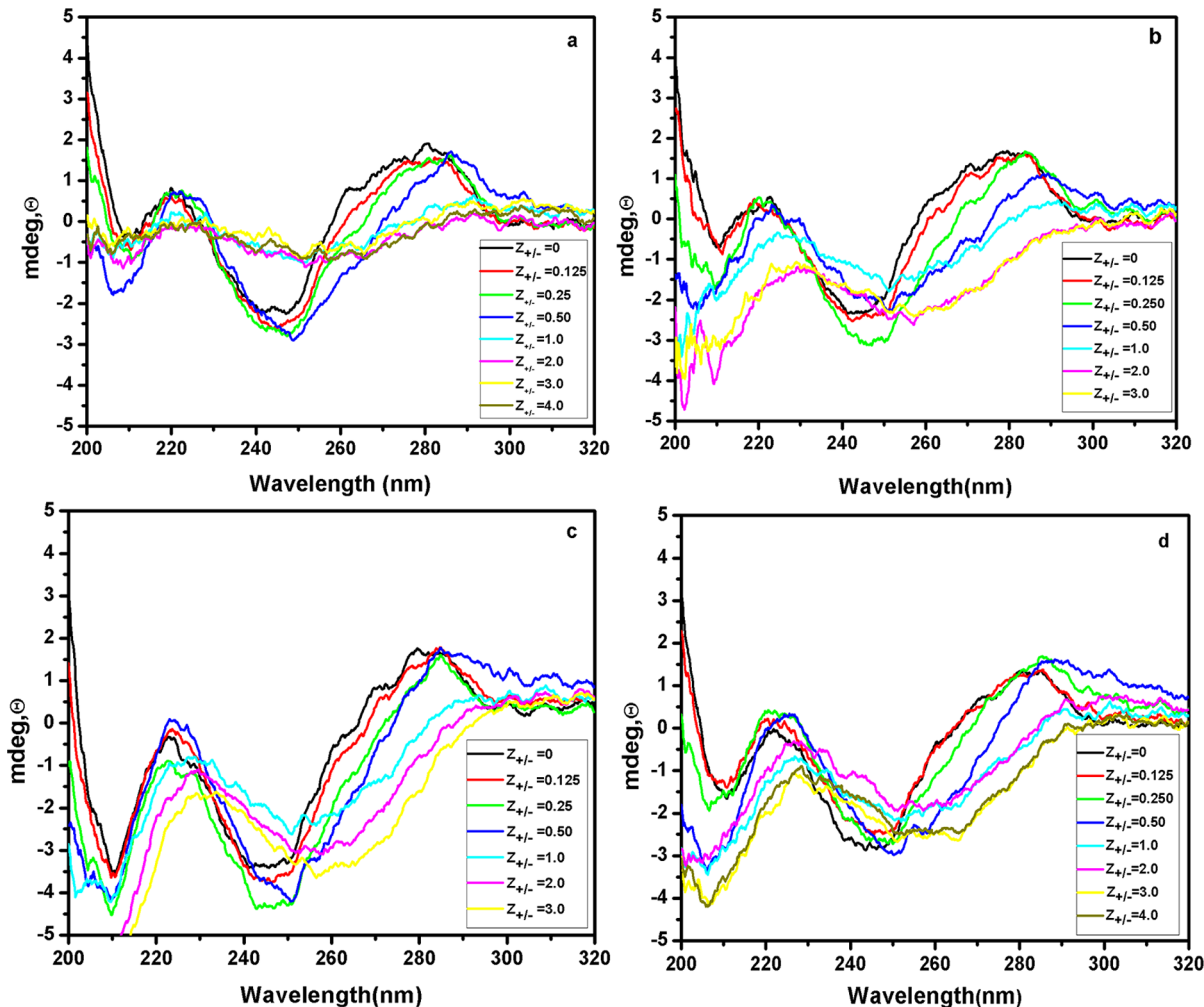


Figure 8. CD spectra of different *ct*DNA–BCP polyplexes at different charge ratios $Z_{+/-}$: (a) PMAPTAC; (b) BCP 90; (c) BCP 63; (d) BCP 37.

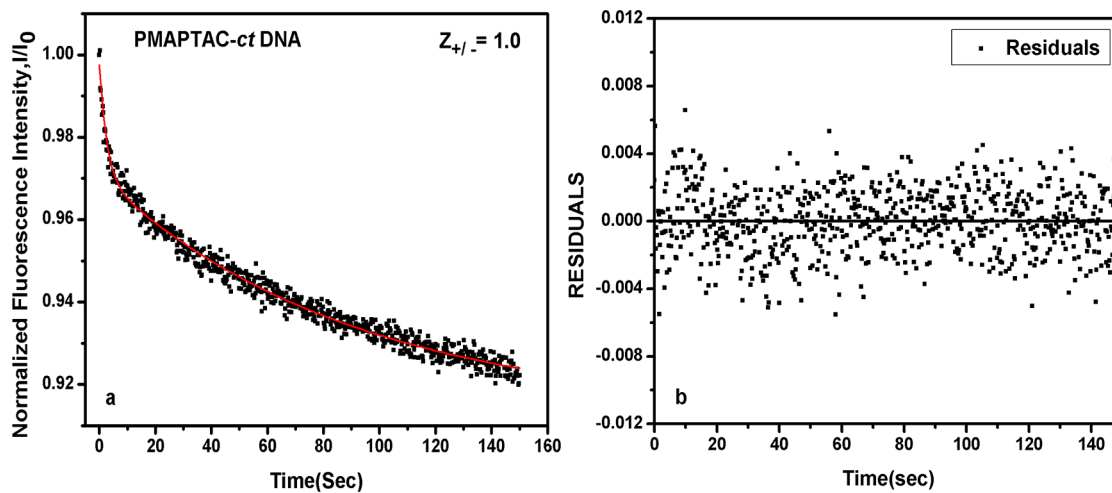


Figure 9. (a) Stopped-flow fluorescence intensity decay of *ct*DNA–PMAPTAC binding at $Z_{+/-} = 1.0$ as a function of time. The smooth line in panel a shows the fitting obtained with eq 2. The residuals of the fit are shown in part b.

into a more condensed state and (ii) dissociation of the DNA–polycation complexes in the cytoplasm of the target cell.^{42–44} In the present investigation, we have used the stopped-flow fluorescence technique to study the kinetics of the interaction of *ct*DNA with the BCPs. Besides the effect of copolymer composition, we have also studied the effect of the charge ratio

on the kinetics of complexation. The observed fluorescence kinetic curves were complex in nature, indicating the possibility of the presence of multiple steps. We postulated that the fluorescence decay curves are a superposition of exponential terms:

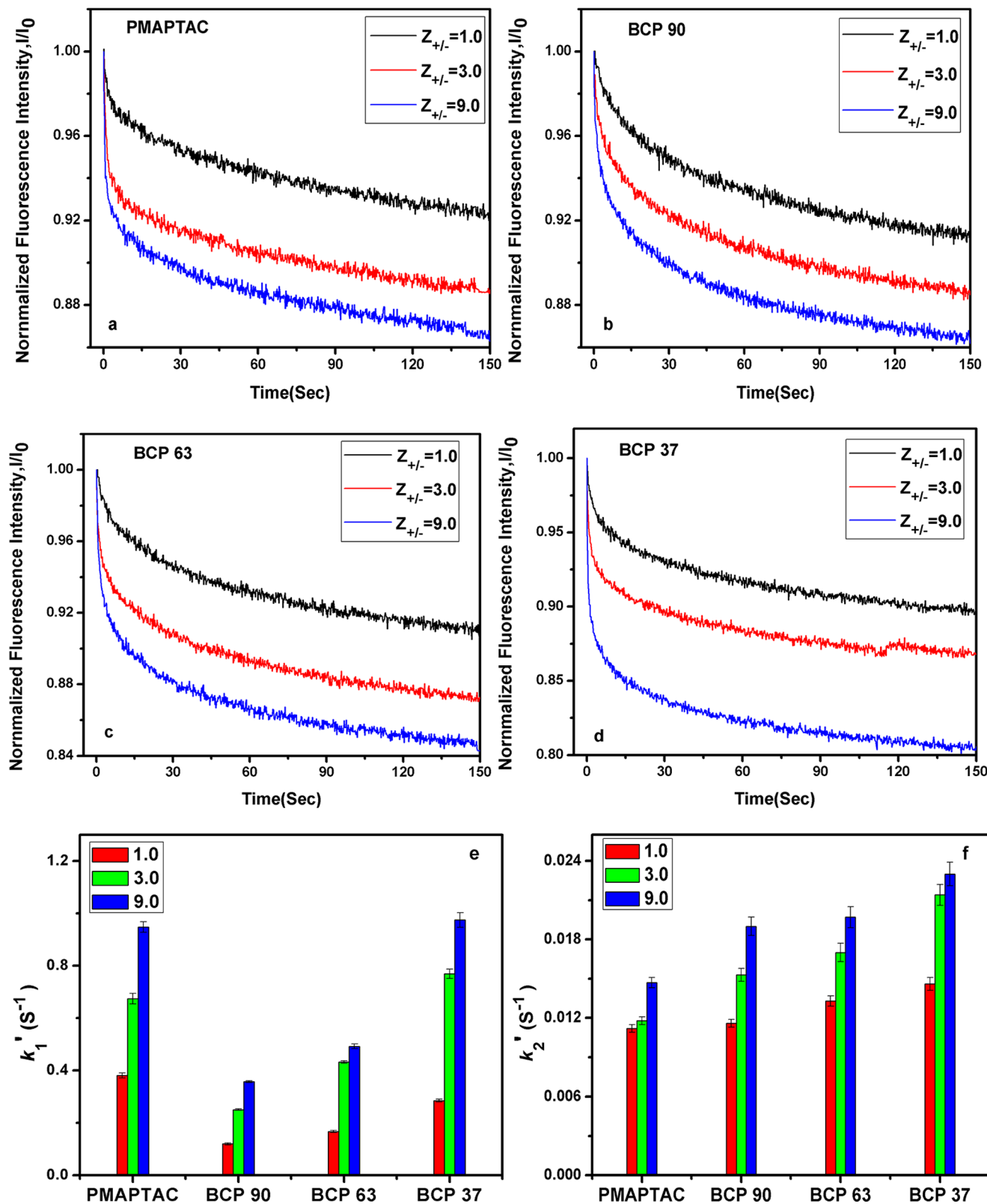


Figure 10. Fluorescence intensity of the ctDNA–EB complex as a function of time after mixing with BCPs at different BCP to ctDNA charge ratios ($Z_{+/-} = 1.0, 3.0$, and 9.0): (a) PMAPTAC; (b) BCP 90; (c) BCP 63; (d) BCP 37. Parts e and f show a comparison of rate constants in the case of different BCPS at different charge ratios.

$$I(t) = \sum A_i \exp(-t/\tau_i) \quad (2)$$

where $I(t)$ is the fluorescence at time t , A_i is the prefactor, and τ_i is the pseudo-first-order time constant. The reciprocal of the

time constant is the rate constant k_i of the reaction. The Nelder–Mead simplex method for minimizing eq 2 was applied. The quality of the fits was assessed from the χ^2 value. Data analysis was performed using Origin 8.0 software.

Kinetic data were fitted by a nonlinear least-squares method to a biexponential relationship. Figure 9a shows a typical fluorescence intensity decay of EB observed upon PMAPTAC homopolymer binding to *c*tDNA at $Z_{+/-} = 1.0$ in 10 mM phosphate buffer solution. The kinetic curves showed multi-exponential decay and were analyzed by fitting them to a sum of exponentials (eq 2). The number of exponentials was increased until no systematic deviation of the residual was found (as shown in Figure 9b). Two exponentials were necessary to fit the data for this particular case. Figure 10 shows experimental plots of EB fluorescence intensity as a function of time for each of the three cationic BCPs and PMAPTAC at three different charge ratios ($Z_{+/-} = 1.0, 3.0, 9.0$) at 25 °C. The fluorescence decay curves were fitted to eq 2. Table 3 shows the

Table 3. Relative Rate Constants for the Binding of Different Cationic BCPs to *c*tDNA as a Function of Charge Ratio, $Z_{+/-}$, at a Fixed Concentration of *c*tDNA and Temperature

cationic polymer	charge ratio ($Z_{+/-}$)	$k_1 \times 10^1$ (s^{-1})	$k_2 \times 10^2$ (s^{-1})
PMAPTAC	1.0	3.81 ± 0.10	1.12 ± 0.03
	3.0	6.74 ± 0.20	1.18 ± 0.03
	9.0	9.48 ± 0.20	1.47 ± 0.04
BCP 90	1.0	1.20 ± 0.04	1.16 ± 0.03
	3.0	2.50 ± 0.03	1.53 ± 0.05
	9.0	3.57 ± 0.04	1.90 ± 0.07
BCP 63	1.0	1.67 ± 0.04	1.33 ± 0.04
	3.0	4.32 ± 0.05	1.70 ± 0.07
	9.0	4.92 ± 0.09	1.97 ± 0.08
BCP 37	1.0	2.85 ± 0.06	1.46 ± 0.05
	3.0	7.69 ± 0.18	2.14 ± 0.08
	9.0	9.75 ± 0.28	2.30 ± 0.09

reciprocal of the time constants as a function of $Z_{+/-}$ for the different cationic BCPs at constant DNA concentration and temperature. Each rate constant is the average of three independent experiments. As previously reported,^{45–47} these time constants are relative in nature with their reciprocals being equal to rate constant values. The rate constant values were found to be well separated, by at least an order of magnitude, for all the cationic BCPs under investigation. The reaction followed a bimolecular mechanistic pathway. From the exponential plots, we obtained the two time constants of the reaction. The relative rate constants followed the order $k'_1 > k'_2$. All fluorescence emission decay curves fit into the biexponential function, indicating a two-step process. In general, it was observed that the initial step was very fast in all of the cases, corresponding to a completely electrostatic driven process. k'_1 increased with an increase in the charge ratio $Z_{+/-}$. The second step was a slower one compared to the first one, where condensation of DNA occurred with a simultaneous internal rearrangement of the *c*tDNA–BCP complex.^{45–47} The k'_2 values also increased with an increase in $Z_{+/-}$, although the increase was lesser compared to k'_1 . This is expected because, in the second step involving compaction of DNA, the electrostatic binding force is not the sole factor.

■ DISCUSSION

In this work, the interactions between three synthesized BCPs and *c*tDNA were investigated using UV spectra, turbidity measurement, EB dye displacement, CD spectra, gel electrophoresis, and UV melting experiments. In addition to these, we have performed stopped-flow kinetic studies for understanding

the mechanism by which the kinetic factors govern the compaction process of DNA that finally leads to the formation of stable polyplexes. Similar binding kinetics studies have been done earlier with commercially available PAMAM dendrimers and synthesized surfactants.^{45–47} From UV studies (Figure 2), it may be predicted that the cationic BCPs bind with *c*tDNA through electrostatic interactions, the cationic charges of MAPTAC units binding with the negatively charged phosphate groups of *c*tDNA that finally leads to charge neutralization of the DNA backbone. The PEG block length of the three BCPs used in this study was the same, and the cationic PMAPTAC block length was varied. In our experiments, we have followed the titrimetric method with respect to $Z_{+/-}$ ratio. That means, at the same charge ratio $Z_{+/-}$, we were adding different amounts of PEGs in DNA solution depending upon BCP composition.

The binding ability of BCPs and PMAPTAC with DNA was monitored by recording the fluorescence of *c*tDNA–EB complexes (Figure 3 and Figure S4, Supporting Information). Intercalation of EB into the DNA helix is accompanied by an increase in the fluorescence of this probe. It is known that the addition of any cationic agent (e.g., multivalent cations, surfactants, or polymers) in the DNA–EB complex results in displacement of EB from the intercalated DNA accompanied by quenching of the fluorescence. In the present work, this intercalated EB dye displacement mechanism is the same for all of the BCPs including PMAPTAC. Until the negative charges present on the phosphate groups of DNA backbones are neutralized completely, significant interaction continued to happen between the cationic block (PMAPTAC) and DNA. Once the charge neutralization process is over at higher charge ratio, the local concentration of PEG units around the DNA moiety get increased. Thus, now PEG residues may interact with hydrophobic DNA base pairs. Therefore, PEG might additionally participate in the condensation process in a synergistic manner. PEG is also known for such DNA condensing ability.^{48,49} More condensation of DNA chains occurs, resulting in release of the rest of the intercalated EB molecules from DNA.

UV melting data showed (Figure 4 and Figure S6, Supporting Information) the presence of free DNA (melting point ~73 °C) and polyplexes with higher melting point (beyond the highest accessible temperature of the experiment). With increasing $Z_{+/-}$, the fraction of free DNA in the mixture decreased and, as a result, the absorbance value after melting also decreased. In the literature, a similar kind of behavior has also been reported for this kind of polyelectrolyte systems.^{41,50} UV melting studies showed that DNA present in a polymer bound state is more stable than the free native state. The strong electrostatic interaction between positively charged units of BCPs and negatively charged phosphate groups of DNA led to the reduction in the electrostatic repulsion among the phosphate groups of the DNA backbone, thus increasing the stability of the DNA helical structures of DNA.⁵¹ For the control experiment, we have compared DNA melting profiles in the presence of PEGMC (PEG macro CTA) also, which is present in every synthesized BCP. In PEGMC, there is no charged group present; hence, the stabilizing electrostatic effect is absent during binding with native DNA. Rather, charged phosphate groups of DNA that are surface exposed try to repel PEG chains, resulting in slight destabilization of the DNA. In the case of BCPs, for a given $Z_{+/-}$, in addition to electrostatic attractive forces, the hydrophobic interactions between PEG

chains and DNA base pairs become significant enough at close proximity of the two macromolecules, promoting stronger binding between the two. This result is exactly similar as obtained for the EB dye exclusion experiment (Figure 3).

Figure 5 shows the variation of the average hydrodynamic size at different charge ratios. As mentioned in the Results section, the average sizes obtained could be distinguished into three different regions. Figure 6 shows the size distribution of the polyplexes for the *c*tDNA–PMAPTAC system. It can be observed that a bimodal distribution appears at low to medium charge ratios that becomes monomodal at high charge ratios. The size distributions of the polyplexes for other systems are shown in the Supporting Information (Figure S7a–c). The values of the various sizes are presented in the Supporting Information (Table S1). These distribution profiles clearly suggest that there are two different populations of DNA molecules when cationic BCPs were added to the DNA. As the DNA charge neutralization proceeds, the solution contains a mixture of two polyplexes with two different levels of compaction. The compaction is maximum near charge ratio $Z_{+-} \sim 1$. Above $Z_{+-} \sim 1$, the average size of BCP bound DNA complexes increased drastically to 2000 to 2600 nm at $Z_{+-} \sim 3$ and the distribution was found to be unimodal at higher charge ratios. We believe that, around $Z_{+-} \sim 1$, a significant amount of the DNA chains are compacted in a globular conformation. At higher charge ratios, the interaction among globular compact polyplexes leads toward the formation of globular aggregates of larger sizes. As a result, DNA–polyplex size increases further. Finally, with a further increase in charge ratio above $Z_{+-} = 3$, no appreciable change in the average size of the polymer–DNA complexes was observed. This clearly indicates polymer bound DNA complexes finally transformed into rigid compact globule aggregates that remained unaffected with further addition of any cationic BCPs.

In the gel electrophoresis study (Figure 7), for mixtures with different Z_{+-} , a similar mobility of the DNA bands was observed. The intensity of the bands decreased gradually with an increase in the value of Z_{+-} . These facts indicate the presence of free DNA and neutralized polyplexed DNA in the mixtures at various relative proportions in different charge ratios.^{49,52} With an increase in the Z_{+-} value, the fraction of the free DNA decreased, which resulted in the reduction in band intensity with no change in mobility. For PMAPTAC, the presence of DNA bands even at $Z_{+-} \sim 1.0$ indicates that not all the DNA molecules were neutralized. This may be due to the relatively lower binding affinity of this polymer. At higher charge ratio ($Z_{+-} = 2.0$, lane 7), there was no observable band in the gel, confirming that all the DNA molecules were complexed, leaving no free DNA in the mixture. This inference was also supported by the results from DLS and UV melting study.

CD spectral analysis (Figure 8) shows a remarkable decrease in the positive band in ellipticity at 275 nm with a red shift with an increase in Z_{+-} of the BCPs. Comparative studies suggest that the changes in the peak intensity were sharper in the case of PMAPTAC (no PEG content). Peak intensity variations were found to be lesser in the case of BCP 37 block copolymer. Overall, investigations suggest that the binding of cationic BCPs to negative phosphate groups of *c*tDNA induced minor perturbations in the DNA helical structure up to $Z_{+-} \sim 1.0$, which is true for all BCPs. When the PEG content is higher in the DNA polyplexes, the perturbations in DNA helical structure were resisted to a larger extent. This may be due to the

presence of hydrophobic interactions via long PEG chain and hydrophobic base pair region in DNA in addition to electrostatic binding force.⁴⁸

The complexation process of DNA–cationic agents is a very complicated process. In the literature, equilibrium studies regarding the DNA complexation process have been done more frequently, but the kinetic aspect of the process was mostly ignored/or not studied due to complication involved in the process. Additionally, the fast nature of the process makes it more difficult to study by conventional mixing methods.⁵³ Previous kinetic studies based on the stopped-flow fluorescence method, including studies from our group, concluded at a two-step process of DNA–cationic agents (surfactant, dendrimer) complexation.^{45,47} It may be noted that the values of the rate constants obtained by the stopped-flow dye exclusion methods are relative in nature. As our aim is to investigate whether PMAPTAC homopolymer and PEGylated cationic BCPs kinetically behave in the same manner or differently, determination of the relative rate constants would be very useful.

The binding kinetics studies (Figure 10) showed fluorescence intensity decay of EB-bound *c*tDNA in the presence of different BCPs at different Z_{+-} values. The present system also fits well into the biexponential decay (two-step mechanism). Table 3 indicates the two different relative rate constant values of the binding process at $Z_{+-} = 1.0, 3.0$, and 9.0 , for different sets of synthesized BCPs and PMAPTAC. On plotting the first rate constants k'_1 as a function of Z_{+-} , we observed a steady increase in k'_1 values in the case of all the BCPs as well as PMAPTAC homopolymer. This is expected, as the first step of the DNA binding is a completely electrostatically driven process. At higher Z_{+-} , we added more cationic BCPs to the DNA solution, which promoted a faster interaction, leading to a faster binding. This process is also a diffusion controlled process.⁴⁵ The trend was the same for the second rate constant k'_2 , although the increment was less as compared to the k'_1 values. The second step mainly involved DNA condensation, with the electrostatic binding not being the lone predominating factor. Here compaction of DNA occurred with possible internal rearrangements in DNA secondary structure, which is indeed a slower process compared to the first. It is true that the nature of k'_1 and k'_2 is empirical but still the kinetic study provides sufficient information regarding different binding patterns for BCPs and PMAPTAC.

To explain the effect of architecture and composition of the cationic BCPs on the two rate constants, it is important to remember that PMAPTAC is a cationic homopolymer with no PEG content and, hence, is expected to interact with DNA in a similar manner to any multivalent cation or other polyelectrolyte systems. The BCPs interacted with DNA differently than PMAPTAC due to the presence of PEG units in the polymeric chains. Among the three BCPs studied here, BCP 37 with the highest PEG content exhibited the maximum value for both of the rate constants. This may be attributed to the fact that, at a fixed Z_{+-} , in addition to electrostatic interaction, hydrophobic interaction between the PEG chains and DNA base pairs becomes active in close proximity of two macromolecules. Thus, the rate constant values attained their maximum in the case of BCP with highest PEG content. A comparison of the two rate constants observed in the case of PMAPTAC and the cationic BCPs revealed two opposite trends. In the case of k'_1 , the values decreased from PMAPTAC to the BCPs, suggesting slowing down of the electrostatic

binding process due to the large exclusion volume of PEG chains in aqueous medium. However, k'_2 was seen to increase from PMAPTAC to the BCPs, which may be directly correlated to the PEG content in the polymer chains. Higher PEG content in the cationic blocks helps DNA to condense more as compared to the homopolymer PMAPTAC with no PEG content. Dominant hydrophobic interactions between two macromolecules at close proximity in the compact state of DNA may be responsible for this.

CONCLUSIONS

We have successfully synthesized a series of cationic block copolymers by polymerizing MAPTAC in the presence of PEG macro chain transfer agent via the RAFT polymerization technique. Although all of the cationic BCPs can effectively bind with calf-thymus DNA through electrostatic binding interactions, the blocks with higher PEG content showed slightly more binding toward DNA. The reinforcing hydrophobic interactions between PEG chains of the BCPs and the DNA base pairs contributed to the preferential binding in addition to the normal electrostatic interactions present in the system. Further, an investigation into the binding kinetics by the stop-flow technique revealed the same trend as that of the steady state equilibrium study. All of the BCPs are capable of forming soluble condensed DNA polyplexes even at higher charge ratios. We believe that these synthesized PEG based cationic block copolymers have attractive potential to work as vehicles in nonviral gene delivery research.

ASSOCIATED CONTENT

Supporting Information

¹H NMR of the CTA and other BCPs, EB-exclusion plots, UV melting profiles of BCPs at various charge ratios, and DLS histograms for BCPs. This material is available free of charge via the Internet at <http://pubs.acs.org>.

AUTHOR INFORMATION

Corresponding Author

*E-mail: dibakar@chem.iitkgp.ernet.in, dibakar@live.in. Phone: +91-3222-282326. Fax: +91-3222-282252.

Notes

The authors declare no competing financial interest.

ACKNOWLEDGMENTS

Financial support from SRIC, Indian Institute of Technology Kharagpur (project code ADA, institute approval number - IIT/SRIC/CHY/ADA/2014-15/18) is acknowledged. D.D. and R.B. acknowledge UGC, New Delhi, for Senior Research Fellowships.

REFERENCES

- (1) Alton, E.; Ferrari, S.; Griesenbach, U. Progress and Prospects: Gene Therapy Clinical Trials (part 1). *Gene Ther.* **2007**, *14*, 1439–1447.
- (2) Alton, E.; Ferrari, S.; Griesenbach, U. Progress and Prospects: Gene therapy Clinical Trials (part 2). *Gene Ther.* **2007**, *14*, 1555–1563.
- (3) Li, S. D.; Huang, L. Non-viral is Superior to Viral Gene Delivery. *J. Controlled Release* **2007**, *123*, 181–183.
- (4) Anderson, W. F. Human Gene Therapy. *Science* **1992**, *256*, 808–813.
- (5) Zuber, G.; Dauty, E.; Nothisen, M.; Belguisse, P.; Behr, J. P. Towards Synthetic Viruses. *Adv. Drug Delivery Rev.* **2001**, *52*, 245–253.
- (6) Park, T. G.; Jeong, J. H.; Kim, S. W. Current status of polymeric gene delivery systems. *Adv. Drug Delivery Rev.* **2006**, *58*, 467–486.
- (7) Mintzer, M. A.; Simanek, E. E. Nonviral Vectors for Gene delivery. *Chem. Rev.* **2009**, *109*, 259–302.
- (8) Jeong, J. H.; Kim, S. W.; Park, T. G. Molecular Design of Functional Polymers for Gene Therapy. *Prog. Polym. Sci.* **2007**, *32*, 1239–1274.
- (9) Gebhart, C. L.; Kabanov, A. V. Evaluation of Polyplexes as Gene Transfer Agents. *J. Controlled Release* **2001**, *73*, 401–416.
- (10) Wagner, E. Strategies to Improve DNA Polyplexes for in vivo Gene Transfer: Will “Artificial viruses” be the Answer? *Pharm. Res.* **2004**, *21*, 8–14.
- (11) Nisha, C. K.; Manorama, S. V.; Ganguli, M.; Maiti, S.; Kizhakkedathu, J. N. Complexes of Poly(ethylene glycol)-Based Cationic Random Copolymer and Calf Thymus DNA: A Complete Biophysical Characterization. *Langmuir* **2004**, *20*, 2386–2396.
- (12) Van de Wetering, P.; Schuurmans-Nieuwenbroek, W. E.; Hennink, W. E.; Storm, G. Comparative Transfection Studies of Human Ovarian Carcinoma Cells in vitro, ex vivo and in vivo with Poly-(2-N-(dimethyl amino ethyl methacrylate)-based Polyplexes. *J. Gene Med.* **1999**, *1*, 156–165.
- (13) Andersson, T.; Aseyev, V.; Tenhu, H. Complexation of DNA with Poly(methacryloxy ethyl trimethylammonium chloride) and Its Poly(oxyethylene) Grafted Analogue. *Biomacromolecules* **2004**, *5*, 1853–1861.
- (14) Kircheis, R.; Wagner, E. Polycation/DNA Complexes For in Vivo Gene Delivery. *Gene Ther. Regul.* **2000**, *1*, 95–114.
- (15) Ochietti, B.; Guerin, N.; Vinogradov, S. V.; St-Pierre, Y.; Lemieux, P.; Kabanov, A. V.; Alakhov, V. Y. Altered Organ Accumulation of Oligonucleotides Using Polyethyleneimine Grafted with Poly(ethyleneoxide) or Pluronic as Carriers. *J. Drug Targeting* **2002**, *10*, 113–121.
- (16) Funhoff, A. M.; Van Nostrum, C. F.; Koning, G. A.; Schuurmans- Nieuwenbroek, N. M. E.; Crommelin, D. J. A.; Hennink, W. E. Endosomal Escape of Polymeric Gene Delivery Complexes Is Not Always Enhanced by Polymers Buffering at Low pH. *Biomacromolecules* **2004**, *5*, 32–39.
- (17) Smedt, S. D.; Demeester, J.; Hennink, W. Cationic Polymer Based Gene Delivery Systems. *Pharm. Res.* **2000**, *5*, 1425–1433.
- (18) Rolland, A. Gene medicines: The End of The Beginning? *Adv. Drug Delivery Rev.* **2005**, *57*, 669–673.
- (19) Boussif, O.; Lezoualch, F.; Zanta, M. A.; Mergny, M. D.; Scherman, D.; Demeneix, B. A Versatile Vector for Gene and Oligonucleotide Transfer into Cells in Culture and in Vivo: Polyethylenimine. *Proc. Natl. Acad. Sci. U.S.A.* **1995**, *92*, 7297–7301.
- (20) Chen, W.; Turro, N. J.; Tomalia, D. A. Using Ethidium Bromide To Probe the Interactions between DNA and Dendrimers. *Langmuir* **2000**, *16*, 15–19.
- (21) Smedt, S. D.; Demeester, J.; Hennink, W. E. Cationic Polymer Based Gene Delivery Systems. *Pharm. Res.* **2000**, *17*, 113–126.
- (22) Bronich, T. K.; Ngueyen, H. K.; Eisenberg, A.; Kabanov, A. V. Recognition of DNA Topology in Reactions between Plasmid DNA and Cationic Copolymers. *J. Am. Chem. Soc.* **2000**, *122*, 8339–8343.
- (23) Tseng, W. C.; Jong, C. M. Improved Stability of Polycationic Vector by Dextran-Grafted Branched Polyethylenimine. *Biomacromolecules* **2003**, *4*, 1277–1284.
- (24) Oupicki, D.; Ogris, M.; Howard, K. A.; Dash, P. R.; Ulbrich, K.; Seymour, L. W. Importance of Lateral and Steric Stabilization of Polyelectrolyte Gene Delivery Vectors for Extended Systemic Circulation. *Mol. Ther.* **2002**, *5*, 463–472.
- (25) Piroton, S.; Muller, C.; Pantoustier, N.; Botteman, F.; Collinet, S.; Grandfils, C.; Dandrifosse, G.; Degée, P.; Dubois, P.; Raes, M. Enhancement of Transfection Efficiency Through Rapid and Non-covalent Post-PEGylation of Poly(dimethylaminoethyl methacrylate)/DNA complexes. *Pharm. Res.* **2004**, *21*, 1471–1479.

- (26) Kabanov, A. V. Taking Polycation Gene Delivery Systems from In Vitro to In Vivo. *Pharm. Sci. Technol. Today* **1999**, *2*, 365–372.
- (27) Braunecker, W. A.; Matyjaszewski, K. Controlled/Living Radical Polymerization: Features, Developments, and Perspectives. *Prog. Polym. Sci.* **2007**, *32*, 93–146.
- (28) Moad, G.; Rizzardo, E.; Thang, S. H. Reversible Addition Fragmentation Chain Transfer (RAFT) Polymerization. *Mater. Matter.* **2010**, *S*, 2–4.
- (29) Chieffari, J.; Chong, Y. K.; Ercole, F.; Krstina, J.; Jeffery, J.; Le, T. P. T. Living Free Radical Polymerization by Reversible Addition-Fragmentation Chain Transfer The RAFT Process. *Macromolecules* **1998**, *31*, 5559–5562.
- (30) Pena, A. M. D. L.; Mansilla, A. E.; Pulgarin, J. A.; Molina, A. A.; Lopez, P. F. Stopped-flow Determination of Dipyridamole in Pharmaceutical Preparations by Micellar-Stabilized Room Temperature Phosphorescence. *Talanta* **1999**, *48*, 1061–1073.
- (31) Stenzel, M. H.; Davis, T. P.; Fane, A. G. Honeycomb Structured Porous Films Prepared from Carbohydrate Based Polymers Synthesized via The RAFT Process. *J. Mater. Chem.* **2003**, *13*, 2090–2097.
- (32) Venkataraman, S.; Ong, W. L.; Ong, Z. Y.; Loo, S. C. J.; Rachel, E. P. L.; Yang, Y. Y. The Role of PEG Architecture and Molecular Weight in the Gene Transfection Performance of PEGylated Poly(dimethylaminoethyl methacrylate) Based Cationic Polymers. *Biomaterials* **2011**, *32*, 2369–2378.
- (33) Banerjee, R.; Gupta, S.; Dey, D.; Maiti, S.; Dhara, D. Synthesis of PEG Containing Cationic Block Copolymers and their Interaction with Human Serum Albumin. *React. Funct. Polym.* **2014**, *74*, 81–89.
- (34) Tonomura, B.; Nakatani, H.; Ohnishi, M.; Yamaguchiito, J.; Hiromi, K. Test Reactions for a Stopped-flow Apparatus - Reduction of 2, 6-dichlorophenolindophenol and Potassium ferricyanide by L-Ascorbic acid. *Anal. Biochem.* **1978**, *84*, 370–383.
- (35) Ottaviani, M. F.; Furini, F.; Casini, A.; Turro, N. J.; Jockusch, S.; Tomalia, D. A.; Messori, L. Formation of Supramolecular Structures between DNA and Starburst Dendrimers Studied by EPR, CD, UV and Melting Profiles. *Macromolecules* **2000**, *33*, 7842–7851.
- (36) Rajendran, A.; Nair, B. U. Unprecedented Dual Binding Behaviour of Acridine Group of Dye: A Combined Experimental and Theoretical Investigation for the Development of Anticancer Chemotherapeutic Agents. *Biochim. Biophys. Acta* **2006**, *1760*, 1794–1801.
- (37) Ivanov, V. I.; Minchenkova, L. E.; Schyolkina, A. K.; Poletayer, A. I. Different Conformations of Double Stranded Nucleic acid in Solution as Revealed by Circular Dichroism. *Biopolymer* **1973**, *12*, 89–110.
- (38) Jing, B.; Dong, J.; Li, J.; Xu, T.; Li, L. Synthesis, Crystal Structure, and DNA Interaction of an Oxovanadium(IV) Complex Containing L-valine Schiff Base and 1,10-Phenanthroline. *J. Coord. Chem.* **2013**, *66*, 520–529.
- (39) Schallon, A.; Synatschke, C. V.; Pergushov, D. V.; Jerome, V.; Muller, A. H. E.; Freitag, R. DNA Melting Temperature Assay for Assessing the Stability of DNA Polyplexes Intended for Nonviral Gene Delivery. *Langmuir* **2011**, *27*, 12042–12051.
- (40) Breslauer, K. J. Extracting Thermodynamic Data from Equilibrium Melting Curves for Oligonucleotide Order-Disorder Transitions. *Methods Enzymol.* **1995**, *259*, 221–242.
- (41) Katayose, S.; Kataoka, K. Water-Soluble Polyion Complex Associates of DNA and Poly(ethylene glycol)-Poly(L-lysine) Block Copolymer. *Bioconjugate Chem.* **1997**, *8*, 702–707.
- (42) Dias, R. S.; Lindman, B. *DNA Interactions with Polymers and Surfactants*; John Wiley & Sons: Hoboken, NJ, 2008.
- (43) Godbey, W. T.; Mikos, A. G. Recent Progress in Gene Delivery Using Non-viral Transfer Complexes. *J. Controlled Release* **2001**, *72*, 115–125.
- (44) Ilarduya, C. T. D.; Sun, Y.; Düzunges, N. Gene Delivery by Lipoplexes and Polyplexes. *Eur. J. Pharm. Sci.* **2010**, *40*, 159–170.
- (45) Santhiya, D.; Dias, R. S.; Dutta, S.; Das, P. K.; Miguel, M. G.; Lindman, B.; Maiti, S. Kinetic Studies of Amino Acid-Based Surfactant Binding to DNA. *J. Phys. Chem. B* **2012**, *116*, 5831–5837.
- (46) Barreiro, P. C. A.; Lindman, B. The Kinetics of DNA-Cationic Vesicle Complex Formation. *J. Phys. Chem. B* **2003**, *107*, 6208–6213.
- (47) Dey, D.; Kumar, S.; Maiti, S.; Dhara, D. Stopped-Flow Kinetic Studies of Poly(amidoamine) Dendrimers-Calf Thymus DNA to Form Dendriplexes. *J. Phys. Chem. B* **2013**, *117*, 13767–13774.
- (48) Froehlich, E.; Mandeville, J. S.; Arnold, D.; Kreplak, L.; Tajmir-Riahi, H. A. PEG and mPEG-Anthracene Induce DNA Condensation and Particle Formation. *J. Phys. Chem. B* **2011**, *115*, 9873–9879.
- (49) Petersen, H.; Fechner, P. M.; Martin, A. L.; Kunath, K.; Stolnik, S.; Roberts, C. J.; Fischer, D.; Davies, M. C.; Kissel, T. Polyethylenimine-graft-Poly(ethylene glycol) Copolymers: Influence of Copolymer Block Structure on DNA Complexation and Biological Activities as Gene Delivery System. *Bioconjugate Chem.* **2002**, *13*, 845–854.
- (50) Maruyama, A.; Watanabe, H.; Ferdous, A.; Katoh, M.; Ishihara, T.; Akaike, T. Characterization of Interpolyelectrolyte Complexes between Double-Stranded DNA and Polylysine Comb-Type Copolymers Having Hydrophilic Side Chains. *Bioconjugate Chem.* **1998**, *9*, 292–299.
- (51) Wolf, B.; Hanlon, S. Structural Transitions of Deoxyribonucleic Acid in Aqueous Electrolyte Solutions. II. The Role of Hydration. *Biochemistry* **1975**, *14*, 1661–1670.
- (52) Sharma, R.; Lee, J. S.; Bettencourt, R. C.; Xiao, C.; Konieczny, S. F.; Won, Y. Y. Effects of the Incorporation of a Hydrophobic Middle Block into a PEG-Polycation Diblock Copolymer on the Physicochemical and Cell Interaction Properties of the Polymer-DNA Complexes. *Biomacromolecules* **2008**, *9*, 3294–3307.
- (53) Lim, K. B.; Pardue, H. L. Error-Compensating Kinetic Method for Enzymatic Determinations of DNAs. *Clin. Chem.* **1993**, *39*, 1850–1856.